



HAL
open science

Influence of rapid thermal annealing temperature on the photoluminescence of Tb ions embedded in silicon nitride films

M.M. M Klak, G. Zatoryb, L.W. W Golacki, P. Benzo, C. Labbe, J. Cardin, J. Misiewicz, F. Gourbilleau, A. Podhorodecki

► **To cite this version:**

M.M. M Klak, G. Zatoryb, L.W. W Golacki, P. Benzo, C. Labbe, et al.. Influence of rapid thermal annealing temperature on the photoluminescence of Tb ions embedded in silicon nitride films. *Thin Solid Films*, 2019. hal-02045420

HAL Id: hal-02045420

<https://hal.science/hal-02045420>

Submitted on 22 Feb 2019

HAL is a multi-disciplinary open access archive for the deposit and dissemination of scientific research documents, whether they are published or not. The documents may come from teaching and research institutions in France or abroad, or from public or private research centers.

L'archive ouverte pluridisciplinaire **HAL**, est destinée au dépôt et à la diffusion de documents scientifiques de niveau recherche, publiés ou non, émanant des établissements d'enseignement et de recherche français ou étrangers, des laboratoires publics ou privés.

Influence of rapid thermal annealing temperature on the photoluminescence of Tb ions embedded in silicon nitride films

M.M. Klak^a, G. Zatryb^{a,*}, L.W. Golacki^a, P. Benzo^b, C. Labbé^b, J. Cardin^b, J. Misiewicz^a, F. Gourbilleau^b, A. Podhorodecki^{a,*}

^a Department of Experimental Physics, Faculty of Fundamental Problems of Technology, Wrocław University of Science and Technology, 50-370 Wrocław, Poland

^b CIMAP CNRS/CEA/ENSICAEN/Normandie Université, 6 Bd Maréchal Juin, 14050 Caen Cedex, France

ARTICLE INFO

Keywords:

Terbium
Silicon
Nitride
Excitation
Lifetime
Defects

ABSTRACT

In this work, silicon nitride films containing terbium were deposited by reactive magnetron co-sputtering in a nitrogen enriched plasma and subjected to rapid thermal annealing treatments. The influence of annealing temperature on the emission and absorption properties of these films was investigated by photoluminescence, photoluminescence decay and photoluminescence excitation measurements. An increase in the photoluminescence intensity and photoluminescence decay time was observed upon annealing for the main $^5D_4-^7F_5$ transition of Tb^{3+} ions. This observation was attributed to decrease of the non-radiative recombination and increase of the number of excited Tb^{3+} ions upon annealing. Moreover, high temperature annealing was found to shift the spectral position of absorption bands observed in the photoluminescence excitation spectra. In general, these excitation spectra were shown to have a rather complicated structure and were decomposed into three Gaussian bands. It was suggested that two of these excitation bands might be due to indirect excitation of Tb^{3+} ions via defects and the third excitation band could be due to direct 4f-5d transition.

1. Introduction

Silicon nitride films have been extensively studied in recent years as a promising material for a wide variety of applications in the microelectronic industry, including use as the gate dielectric in field effect and thin film transistors [1], an important antireflection coating layer for crystalline silicon solar cells [2], a charge storage layer in MNOS non-volatile memories [3] and as an active material for light emitting diodes (LEDs) [4]. Research on this material has been additionally stimulated by its full compatibility with Si-based transistor technology, which could lead to easy integration with various microelectronic devices. Among Si-based films designated for application in light sources, rare earth (RE) doped SiN_x structures have received considerable attention, owing to the interesting optical properties of rare earth elements. Up to now, most research in this field has focused on Er, Nd and Yb doped SiN_x films [2,5–7], obtained either by plasma-enhanced chemical vapor deposition (PECVD) or sputtering. For these dopants, efficient near-infrared photoluminescence and electroluminescence have been demonstrated, which is important for telecommunication. Considerably less attention has been paid to other RE dopants, such as Tb, showing emission in the visible range, which is interesting from the

point of view of applications in color LEDs and (when co-doped with Yb) frequency conversion layers for silicon solar cells [2].

The previous studies of Tb-doped SiN_x thin films focused primarily on the influence of film stoichiometry on the Tb photoluminescence intensity [7,8]. In these studies, after deposition films were annealed at high temperatures in conventional furnaces what probably caused their non-intentional oxidation, confirmed by infrared absorption measurements. It is noteworthy that such contamination of Tb: SiN_x films with oxygen can influence optical properties of Tb^{3+} ions, giving rise to a more ionic chemical environment. When analysed from this perspective, it is interesting and important to study non-contaminated Tb: SiN_x films and to test alternative annealing techniques, such as rapid thermal annealing. Moreover, to our knowledge, no systematic experimental study exists which investigates the influence of annealing temperature on the non-radiative recombination of Tb^{3+} ions embedded in SiN_x matrix. Furthermore, while the previous studies emphasized the importance of host-mediated excitation of Tb^{3+} ions in SiN_x matrix [9], there are still many open questions regarding the actual excitation mechanism of Tb^{3+} ions.

In this paper, we investigated the most efficient paths of optical excitation of Tb^{3+} ions embedded in silicon nitride films deposited by

* Corresponding authors.

E-mail addresses: grzegorz.zatryb@pwr.edu.pl (G. Zatryb), artur.p.podhorodecki@pwr.edu.pl (A. Podhorodecki).

reactive magnetron co-sputtering in a nitrogen enriched plasma. The deposited films were subjected to rapid thermal annealing treatments and the temperature allowing to obtain the strongest Tb^{3+} emission intensity was determined. Finally, we discussed the physical mechanism responsible for the observed photoluminescence enhancement of Tb^{3+} ions after high-temperature annealing.

2. Experimental details

The rare earth doped layers have been deposited by co-sputtering reactively a Si and Tb cathodes in a nitrogen-rich plasma. The films were grown on a 2" Si wafer heated at 200 °C and the nitrogen enriched atmosphere was achieved by injecting 8 sccm of Ar and 2 sccm of N in the deposition chamber. The plasma pressure was set at 3 mTorr and the RF power density applied on the Si target was fixed to 4.5 W.cm^{-2} while the optimized RF power density applied on the Tb target was 0.45 W.cm^{-2} . All the deposited layers had a thickness of about 90 nm to avoid any interference effects in the emission spectrum. After deposition, the samples were subjected to rapid thermal annealing (RTA) treatment at different annealing temperatures (T_A), ranging from 600 °C to 1100 °C during 10 min. The composition of the thin layers has been determined by means of RBS measurements as described elsewhere [2]. All the $Tb:SiN_x$ films were found to contain 42.3 at. % of Si, 56.3 at. % of N and 1.4 at. % of Tb. In other words, the chemical composition of films investigated in this study is very close to stoichiometric Si_3N_4 and no oxygen contamination was clearly visible in RBS measurements for the as-deposited films. Nevertheless, since the relative error in determined N concentration is around 6%, a small amount of oxygen contamination cannot be excluded.

The Fourier-transform infrared (FTIR) absorbance spectra were collected using a Nicolet iS10 spectrometer (Thermo Fisher Scientific Instruments). These measurements were conducted in attenuated total reflectance mode (ATR) using a VariGATR accessory with germanium crystal (Harrick Scientific) at an angle of incidence set to 65°. The measured spectra were not corrected for the typical ATR effects e.g. the effect of anomalous dispersion in the vicinity of an absorption peak. For this reason, the ATR absorption peaks may be slightly shifted from their corresponding locations in a transmission spectrum. Here, it is also worth to mention that since the investigated thin films were deposited on Si substrate, our germanium ATR accessory allows to significantly enhance the FTIR signal intensity [10] and should be sensitive to effects such as superficial film oxidation.

Finally, the optical properties of investigated samples were determined by means of photoluminescence (PL), photoluminescence excitation (PLE) and PL decay measurements, conducted at room temperature. For both PL and PLE measurements, the signal emitted from the sample was collected and detected by a Si CCD camera (HR4000 Ocean Optics). For PLE experiments, a continuous wave (cw) xenon lamp connected to a monochromator (Jobin Yvon TRIAX 180) was used as the tunable excitation source. For such measurements, the recorded signal was corrected for the xenon lamp spectral intensity profile. For PL decay measurements, a pulsed excitation line ($\lambda_{\text{exc}} = 266 \text{ nm}$, repetition rate 100 Hz) of an actively Q-switched diode pumped solid state laser (Elforlight Ltd) was used, together with a multichannel detection system equipped with a monochromator and a PMT detector. The detection wavelength ($\lambda_{\text{em}} = 545 \text{ nm}$). The time resolution in all PL decay measurements presented in this study was better than 1 μs . Finally, in the case of cw-PL measurements, the same laser was used for excitation, but the repetition rate was increased to 40 kHz which allowed to operate in quasi-continuous excitation regime.

3. Results and discussion

Fig. 1 shows FTIR absorbance spectra of (a) $Tb:SiN_x$ sample annealed at 1100 °C measured shortly after deposition (b) the same $Tb:SiN_x$ sample after storage in ambient atmosphere for one year and

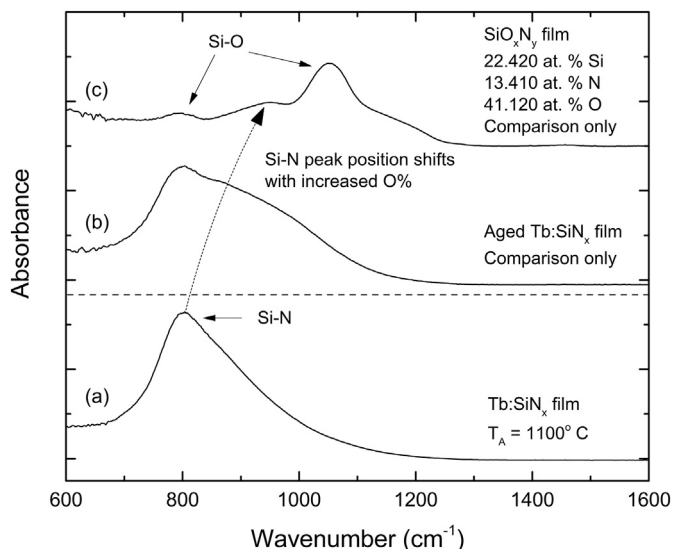


Fig. 1. FTIR absorbance spectra measured for (a) $Tb:SiN_x$ film annealed at 1100 °C shortly after deposition process (b) $Tb:SiN_x$ film annealed at 1100C measured after storage in ambient atmosphere for one year (c) SiO_xN_y film (22.42 at. % Si, 13.410 at. % N and 41.120 at. % O). Spectra (b) and (c) are used only for the purpose of FTIR absorbance discussion and the emission properties of these samples are not the subject of this article. Dashed arrow represents the shift of Si-N absorbance peak and is only a guide to the eye. The spectra were vertically shifted for clarity.

(c) reference SiO_xN_y sample annealed at 1000 °C and containing 22.42 at. % Si, 13.410 at. % N and 41.120 at. % O (this sample is shown for reference purposes only and it was deposited by Plasma Enhanced Chemical Vapor Deposition method as described elsewhere [11]), as determined by RBS measurements. It should be underlined that spectra (b) and (c) are used only for the purpose of FTIR absorbance discussion and the emission properties of these samples are not the subject of this article. It can be seen in Fig. 1 that in the case of spectrum (a) of $Tb:SiN_x$ sample, only one peak can be seen at around 803 cm^{-1} , which is assigned to Si-N asymmetric stretching mode [12,13]. When the annealing temperature increases from 600 to 1100 °C, this peak shifts only slightly, from 799 cm^{-1} to 803 cm^{-1} , indicating a weak bond rearrangement. The broad and asymmetric peak shape is characteristic to silicon nitride and is consistent with reported results for this material [12,14]. Due to the fact that after deposition our samples were stored in ambient atmosphere, it should be noted that Si-O bending mode (796 cm^{-1}) could be superimposed on the Si-N asymmetric stretching mode. Nevertheless, there is no clear signature of the Si-O asymmetric stretching mode at 1058 cm^{-1} in spectrum (a). This suggests that high temperature annealing did not result in film oxidation, as reported in some other studies [7,8]. For comparison, the effect of oxidation is clearly seen in spectrum (b), obtained for the same $Tb:SiN_x$ sample stored in ambient atmosphere for one year. As can be seen, spectrum (b) is far different from spectrum (a): for spectrum (b) two separate peaks can be distinguished at 803 cm^{-1} , assigned to Si-O bending mode, and at 862 cm^{-1} , assigned to Si-N asymmetric stretching mode. Such assignment can be confirmed when looking at spectrum (c) measured for $Si_xO_yN_z$ film. It can be seen that for this silicon oxynitride film there are three distinguishable peaks assigned to Si-O asymmetric stretching mode (1058 cm^{-1}), Si-O bending mode (796 cm^{-1}) and Si-N asymmetric stretching mode at 950 cm^{-1} . Moreover, as can be seen in Fig. 1, the position of Si-N asymmetric stretching mode shifts significantly towards higher wavenumbers when oxygen amount in the silicon-nitride films increases. This observation is consistent with the previous reports stating that Si-N vibrational modes can be found between 490 and 1020 cm^{-1} [15] and their position depends on the oxygen content [16]. Indeed, the dotted arrow drawn on the Fig. 1 shows that Si-N

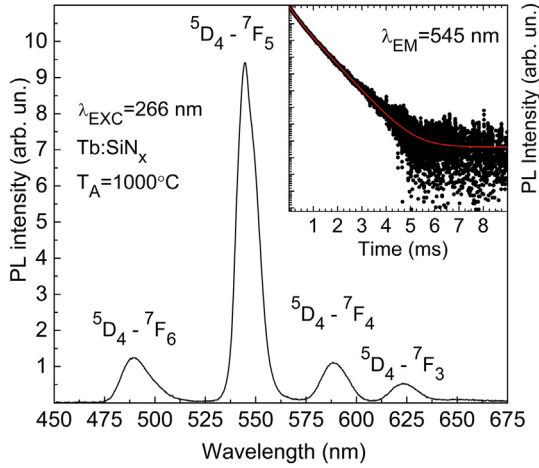


Fig. 2. Room temperature photoluminescence spectrum of Tb:SiN_x film annealed at 1000 °C. The inset shows photoluminescence decay measured for this sample for $^5D_4 \rightarrow ^7F_5$ emission line, together with double-exponential fit.

related peak can be shifted from 803 cm^{-1} to 950 cm^{-1} . Additionally, there is no detectable Si-O asymmetric stretching mode in the spectrum (a) of Tb:SiN_x samples. As demonstrated in spectrum (b) in Fig. 1, our ATR-FTIR measurement technique is sensitive to superficial oxidation of silicon nitride films. Nevertheless, such oxidation has not been clearly detected in any spectra of the samples investigated in this study. Together with RBS data, this result indicates that if there is any oxygen present in the investigated films, its concentration is very low. This is in contrast to some other studies [7,8] where strong signature of Si-O bonds was observed in FTIR spectra of Tb:SiN_x films, most probably as a result of superficial oxidation that took place as soon as the samples were removed at high temperature from the conventional furnace.

Fig. 2 shows a PL spectrum of Tb:SiN_x film annealed at 1000 °C. Four main PL bands can be seen that originate from radiative transitions within the 4f shell of Tb³⁺ ions. The observed transitions are $^5D_4 \rightarrow ^7F_6$ (490 nm), $^5D_4 \rightarrow ^7F_5$ (545 nm), $^5D_4 \rightarrow ^7F_4$ (589 nm) and $^5D_4 \rightarrow ^7F_3$ (623 nm) [17]. The same emission bands were identified also for samples annealed at other temperatures (not shown here). These transitions and their spectral positions are very similar to the emission lines of Tb³⁺ ions embedded in silicon oxide [18], silicon oxynitride [19,20], or silicon carbide films [21] and their overall shape does not change after annealing. Finally, it should be underlined that measured PL spectra did not show any signature of the broad matrix-related PL which has been reported by other authors for undoped SiN_x films [13,22]. Recently, such matrix-related PL superimposed on Tb³⁺ emission lines has been reported by Guerra et al. [9], but it was detectable only at low measurement temperatures ($\leq 250 \text{ K}$) and for 488 nm excitation wavelength, which is almost resonant with 5D_4 level of Tb³⁺ ions. It is noteworthy that this broad emission band was assigned to different radiative defects present in SiN_x matrix. According to Guerra et al. these defects can transfer the excitation energy to nearby Tb³⁺ ions and such process is phonon-mediated. Since at low temperatures the population of phonons decreases, the efficiency of excitation transfer also drops and emission from defects becomes visible.

Next, to study Tb³⁺ emission properties in more details, measurements of photoluminescence decay were conducted for each sample. An example of such PL decay, measured for the most intense $^5D_4 \rightarrow ^7F_5$ PL band ($\lambda_{EM} = 545 \text{ nm}$), has been shown in the inset of Fig. 2 for the sample annealed at 1000 °C. In general, all measured PL decays were slightly non-single-exponential and were fitted with double-exponential decay function $I_{PL}(t) = A_1 \exp(-t/\tau_1) + A_2 \exp(-t/\tau_2)$, where $I_{PL}(t)$ denotes total PL intensity at time t , τ_1 and τ_2 are PL lifetimes and A_1, A_2 are contributing intensity amplitudes. It should be noted that fitting of these PL decays with a single-exponential decay function $I_{PL}(t) = A \exp$

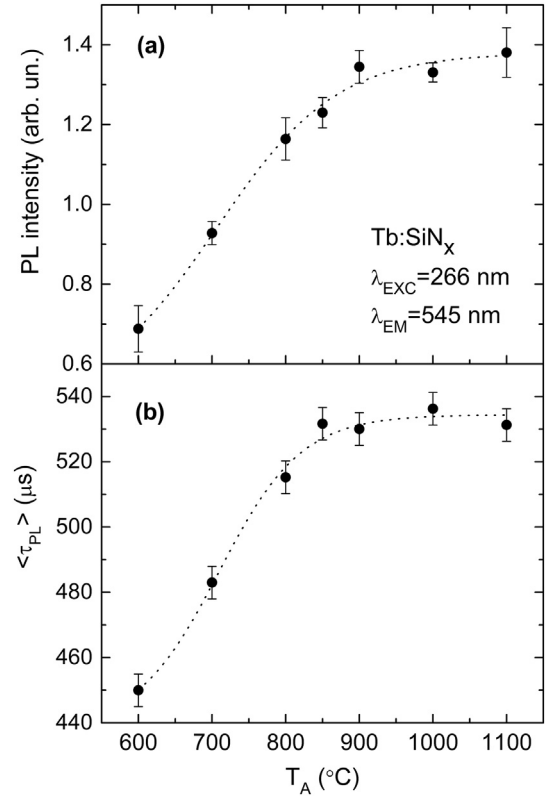


Fig. 3. Photoluminescence intensity (a) and average photoluminescence decay time (b) measured as a function of the annealing temperature for the $^5D_4 \rightarrow ^7F_5$ emission of Tb³⁺ ions. The dotted lines are only a guide to the eye.

($-t/\tau_{PL}$) was also possible but resulted in somewhat lower fit quality at the end of the decay curves. While the obtained PL lifetimes are discussed later, here, it should be underlined that the model selection does not affect any of our later conclusions. Finally, it is worth to mention that similar non-single-exponential shape of PL decay has been also reported for the emission of Yb³⁺ ions embedded in Tb:Yb:SiN_x films [2] or for Al-Tb:SiO₂ multilayers [23]. Unfortunately, we failed to find any reports on the PL decay of Tb³⁺ ions in SiN_x films. Nevertheless, the slightly non-single-exponential character of the PL decay is not unusual and is probably caused by the presence of Tb³⁺ ions at several different sites in the SiN_x matrix.

To study the effect of annealing on the Tb³⁺ PL intensity, the most intense $^5D_4 \rightarrow ^7F_5$ band was chosen to represent the emission of Tb³⁺ ions. For this band, the integrated emission intensity is shown in Fig. 3(a) as a function of annealing temperature. It can be seen that in general annealing treatment results in an increase in the Tb³⁺ PL intensity by up to a factor of 2.0. It should be noted that similar increase in the Tb³⁺ emission intensity after annealing was reported in an earlier study [9], but without mentioning what was the actual composition of Tb:SiN_x films, what makes quantitative comparison difficult. Nevertheless, these results allow us to suspect that the observed temperature tendencies are rather general for Tb³⁺ ions embedded in SiN_x, and that the optimal annealing temperature is around 900 °C because above this temperature PL intensity does not change significantly. Nevertheless, it should be pointed out that the optimal annealing temperature can be different if the annealing conditions change or Tb concentration is different. As shown by Guerra et al. [21] the annealing of Tb-doped thin films is a rather complicated issue and depends on many factors.

To study these annealing effects in more detail, the average PL decay times $\langle \tau_{PL} \rangle$ were calculated for each sample. As it was mentioned before, PL decays were fitted with double-exponential function and for

this reason the average PL lifetime has been defined as $\langle\tau_{PL}\rangle = (A_1\tau_1 + A_2\tau_2)/(A_1 + A_2)$ [24]. Here, it is worth mentioning that for a given PL decay the maximum difference between $\langle\tau_{PL}\rangle$ and $\langle\tau_{PL}\rangle$ calculated from the fit with single-exponential decay function does not exceed 2%. For this reason and to simplify further discussion, we do not assign any physical meaning to τ_1 and τ_2 separately. Nevertheless, we use the interpretation of the average PL lifetime, consistent with the general definition of average surviving time of an excitation. According to this definition, $\langle\tau_{PL}\rangle$ is simply the average amount of time which Tb^{3+} ions spend in their excited 5D_4 states [25]. For this reason, in the simplest case scenario, if there is a non-radiative recombination from 5D_4 excited states of Tb^{3+} ions (such as non-radiative energy transfer to some defect states, energy transfer between Tb^{3+} ions [21,26] or multiphonon relaxation), $\langle\tau_{PL}\rangle$ will become shorter. Strictly speaking, this behavior is expected only when a competition between radiative and non-radiative recombination is possible for 5D_4 excited state. In other words, for 5D_4 excited state, the rate of radiative recombination has to be comparable with the rate of non-radiative recombination. On the other hand, if the non-radiative recombination rate from 5D_4 state is much higher than the radiative recombination rate, a fraction of Tb^{3+} ions becomes non-luminescent (undetectable in PL measurements). In this case, $\langle\tau_{PL}\rangle$ remains constant and a lowered PL intensity is observed.

Fig. 3(b) shows the average PL lifetimes as a function of annealing temperature. It can be seen that the average PL lifetime increases with temperature up to 850 °C and remains fairly constant at around 530 μs for higher temperatures. Such an increase is attributed to a reduction of non-radiative recombination from 5D_4 -excited state and can partly explain the observed enhancement of the PL intensity in that temperature range. However, to first approximation, at low flux of excitation photons ϕ , the PL intensity I_{PL} should increase proportionally to the PL lifetime [27]. In our case, the intensity increases by a factor of 2.0 upon annealing, while $\langle\tau_{PL}\rangle$ increases only by a factor of 1.2. Taking into account that PL intensity I_{PL} does not change proportionally to $\langle\tau_{PL}\rangle$, it is reasonable to suspect that thermal annealing also increases the concentration of excited ions N_{Tb^*} , since $I_{PL} = k_R N_{Tb^*}$. The increase of N_{Tb^*} , could be due to many reasons. For example, annealing treatment could influence the concentration of optically active (available for excitation) ions, by inducing the necessary structural changes of SiN_x matrix, providing the environment for the Tb atoms to be incorporated in their optically-active trivalent state (e.g. from over- or undercoordinated ions to Tb^{3+} [21]). Such mechanism has been reported for Er-implanted semiconductors, where annealing treatment is necessary in order to obtain Er at an optically active site [28,29]. Furthermore, if the excitation of Tb^{3+} ions is indirect, annealing could be responsible for increase of the effective absorption cross-section of Tb^{3+} ions – in such case, the concentration of optically active ions does not have to change, but the number of excited ions N_{Tb^*} should be larger due to more efficient excitation energy transfer from some donor states. Similar mechanism has been reported for Nd^{3+} and Er^{3+} ions embedded in SiO_x matrices [30–32]. Nevertheless, based on the obtained results it is not possible to determine which mechanism is responsible for the increased N_{Tb^*} in our case.

To investigate the excitation mechanism of Tb^{3+} ions, we conducted PLE measurements by monitoring the intensity of main ${}^5D_4 \rightarrow {}^7F_5$ emission band of Tb^{3+} for different excitation wavelengths. The normalized PLE spectra measured for samples annealed at 600 and 1100 °C are shown in Fig. 4. Similar PLE spectra were obtained also for other samples. It can be seen that there are two distinct peaks in the PLE spectra of both samples, which shift to higher energies upon annealing. For both samples, the first peak appears above 4.5 eV, while the second peak appears below 4.5 eV. On closer inspection, it turns out that each PLE spectrum can be fitted with three Gaussians, what suggests presence of at least three different excitation bands of Tb^{3+} ions. An example of such decomposition is shown in Fig. 4. For the purpose of further discussion, each Gaussian component was labeled as B1, B2 and

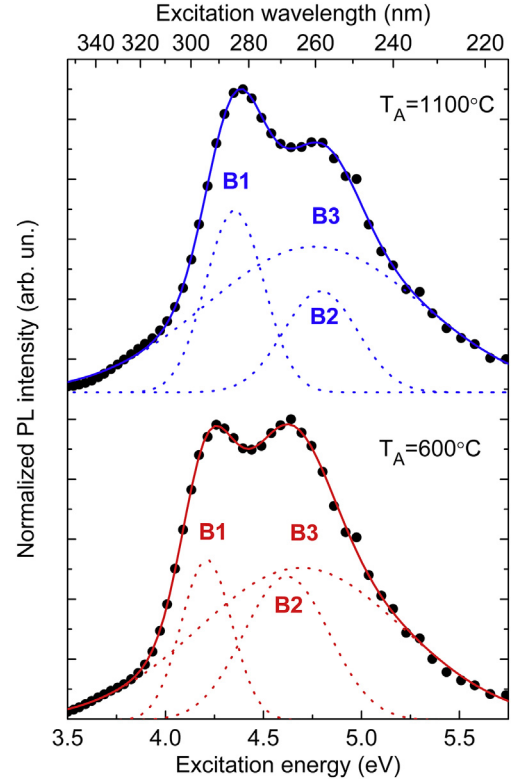


Fig. 4. Normalized photoluminescence excitation spectra (solid dots) measured for ${}^5D_4 \rightarrow {}^7F_5$ emission of $Tb:SiN_x$ films annealed at 600 and 1100 °C. Each spectrum was fitted with three Gaussian components (dotted lines labeled as B1, B2 and B3). The cumulative fits are shown with solid lines.

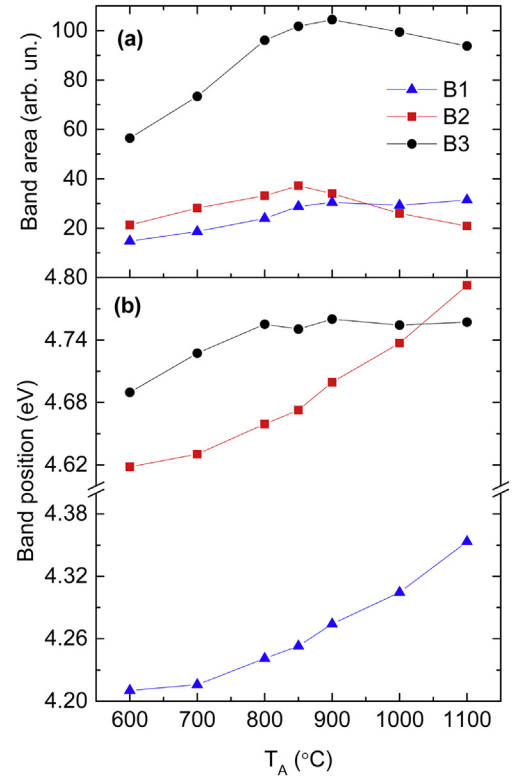


Fig. 5. Integrated band intensity (a) and band peak position (b) obtained for each of the three PLE Gaussian components B1, B2 and B3, shown as a function of the annealing temperature.

B3.

The decomposition of measured PLE spectra into three Gaussian components allows us to make several important observations. First, Fig. 5(a) shows the integrated intensities of bands B1, B2 and B3 as a function of the annealing temperature. It can be seen that in general, the integrated intensities are higher for annealed samples, except for the intensity of band B2 which first increases and then drops above 850 °C. More importantly, according to Fig. 5(a), band B3 almost completely dominates the PLE spectrum, being probably the most efficient excitation channel of Tb^{3+} ions. As a matter of fact, for each annealing temperature, this broad band contains 61–64% of the total integrated PLE intensity.

The second important observation is that in general, the energy of each band maximum shifts upon annealing. As can be seen in Fig. 5(b), the peak position of band B1 and B2 significantly increases as a function of the annealing temperature while the peak position of band B3 increases only slightly up to $T_A = 800$ °C and does not change above this temperature. It is important to underline that the tendency obtained for band B3 is clearly different from the tendencies obtained for band B1 and B2. In particular, the increase of peak energy is 143 meV (3.4%) and 174 meV (3.8%) for band B1 and B2, respectively, and only 68 meV (1.5%) for band B3. Clearly, the peak position of band B1 and B2 is more sensitive to the annealing temperature than the peak position of band B3. This result suggests that mechanism of excitation of Tb^{3+} ions is similar in the case of bands B1 and B2 but different in the case of band B3.

Based on the obtained results, only a tentative explanation of the Tb^{3+} ions excitation mechanism can be given. First, it is important to note that the PLE spectra of Tb^{3+} ions (Fig. 4) show remarkable similarities to PLE spectra of pure silicon nitride films. For example, several broad excitation bands peaking at around 4.2, 4.4, 4.6 and 5.2 eV have been reported for undoped amorphous SiN_x [3,22] films and crystalline Si_3N_4 [4,33], showing that there are optically active states in silicon nitride which have energies in the range of efficient excitation of Tb^{3+} ions. Moreover, as demonstrated by ab initio calculations [34], there are many defects in β - Si_3N_4 with transition levels at 3.1, 3.4, 4.0, 4.5 and 4.6 eV. Similar optical transitions at 3.8–3.85, 4.19–4.27, 4.58 and 4.82 eV were reported for SiN_x films [35] prepared by low-pressure chemical vapor deposition and assigned to defect states. The above examples suggest that indirect excitation of Tb^{3+} ions through some defect states in SiN_x matrix is possible. Taking this into account, we assign bands B1 and B2 to indirect excitation of Tb^{3+} ions through SiN_x defect states. First of all, it is reasonable to expect that the energies of defects should change upon annealing because high temperature treatment induces structural changes in SiN_x matrix. As can be seen in Fig. 5(b), bands B1 and B2 fulfil this criterion and significantly shift after annealing, in contrast to band B3 which moves only slightly. Second, if the excitation transfer occurred from a band tail defect states to some discrete Tb^{3+} states, we would expect to observe an increase of the excitation band position since annealing results in a more ordered silicon nitride network with narrower band tail. Again, this kind of tendency was observed for bands B1 and B2, suggesting indirect excitation of Tb^{3+} ions. Here, it is worth mentioning that the decrease of Urbach energy and simultaneous increase of the Tauc-gap as a function of annealing temperature has been observed before [21] for Tb -doped SiN_x films, which is consistent with our interpretation. Finally, it should be noted that energy of band B1 is close to energies of different defects in SiN_x [34] and the similarity of tendencies obtained for band B1 and B2 suggest rather similar nature of these excitation bands.

As for the band B3, the situation is more complicated. The peak position of band B3 is much less sensitive to T_A and the energy of band maximum at ~ 4.75 eV is close to typical values reported for 4f-5d transitions of Tb^{3+} ions in different host materials [36]. Moreover, 4f-5d transition of Tb^{3+} is known for high absorption cross-section compared to parity forbidden intra-4f shell transitions. Thus, it is possible that band B3 is related to direct excitation of Tb^{3+} ions through 4f-5d

transition. As a matter of fact, this kind of transition was suggested as the excitation mechanism of Tb^{3+} and Ce^{3+} ions in crystalline α - Si_3N_4 powders [37]. From this point of view, the large broadening of B3 could be due to electron-phonon coupling which is usually very strong for f-d transitions [38–40].

In general, our PLE results show that the excitation mechanism of Tb^{3+} ions in SiN_x films is a complicated issue. For this reason, only tentative interpretation of the experimental data is possible at the moment. Finally, we would like to suggest that measurements of PL and PLE as a function of sample temperature could help to clarify this problem in the future. In particular, if the indirect excitation of Tb^{3+} ions is phonon-mediated process, the contribution of respective excitation bands to total PLE spectra should decrease at low temperatures. Moreover, if the band B3 is indeed related to direct 4f-5d transition, the full-width at half maximum (FWHM) of B3 should also decrease at low temperatures [41].

4. Conclusions

In this work, Tb^{3+} -doped SiN_x ($x \approx 4/3$) films were deposited by reactive magnetron co-sputtering in a nitrogen rich plasma and subjected to rapid thermal annealing treatments. It was shown that annealing at elevated temperatures up to 1100 °C influences both absorption and emission properties of these films. In particular, it was found that annealing generally enhances the photoluminescence intensity of Tb^{3+} ions and increases the average photoluminescence decay time measured for the main $^5D_4 \rightarrow ^7F_5$ transition of Tb^{3+} ions. This effect was explained by decrease of the non-radiative recombination rate and increase of the number of excited Tb^{3+} ions upon annealing. Furthermore, according to our results, photoluminescence excitation spectra measured for $^5D_4 \rightarrow ^7F_5$ emission of Tb^{3+} ions show a rather complicated structure with excitation maxima located in the energy range of 4–5 eV. According to our results, these excitation maxima shift to higher energies as a function of the annealing temperature. After decomposition of each photoluminescence excitation spectrum into three Gaussian components it was demonstrated that two excitation bands are especially sensitive to the annealing temperature, suggesting that SiN_x defects might participate in the indirect excitation of Tb^{3+} ions. Nevertheless, the dominant photoluminescence excitation component was shown to be much less sensitive to the annealing temperature what could suggest that excitation of Tb^{3+} ions in SiN_x matrix might occur also as a result of direct 4f-5d transition.

Acknowledgments

In Poland, this work was funded by National Science Centre under Project No.DEC-2012/05/D/ST7/01121.

In France, this work was financially supported by the French Research National Agency through the GENESE project (No ANR-13-BS09-0020-01), and the LABEX EMC3 ASAP project.

References

- [1] S.-J. Tsai, C.-L. Wang, H.-C. Lee, C.-Y. Lin, J.-W. Chen, H.-W. Shiu, L.-Y. Chang, H.-T. Hsueh, H.-Y. Chen, J.-Y. Tsai, Y.-H. Lu, T.-C. Chang, L.-W. Tu, H. Teng, Y.-C. Chen, C.-H. Chen, C.-L. Wu, Approaching defect-free amorphous silicon nitride by plasma-assisted atomic beam deposition for high performance gate dielectric, *Sci. Rep.* 6 (2016) 28326, <https://doi.org/10.1038/srep28326>.
- [2] L. Dumont, J. Cardin, P. Benzo, M. Carrada, C. Labbe, A.L. Richard, D.C. Ingram, W.M. Jadwisieniczak, F. Gourbilleau, $SiN_x:Tb^{3+} + -Yb^{3+}$, an Efficient Down-conversion Layer Compatible With a Silicon Solar Cell Process, (2015), <https://doi.org/10.1016/j.solmat.2015.09.031>.
- [3] V.A. Gritsenko, T.V. Perevalov, O.M. Orlov, G.Y. Krasnikov, Nature of traps responsible for the memory effect in silicon nitride, *Appl. Phys. Lett.* 109 (2016) 62904, <https://doi.org/10.1063/1.4959830>.
- [4] L. Museur, A. Zerr, A. Kanaev, Photoluminescence and electronic transitions in cubic silicon nitride, *Sci. Rep.* 6 (2016) 18523, <https://doi.org/10.1038/srep18523>.
- [5] A.R. Zanatta, M.J.V. Bell, L.A.O. Nunes, Visible photoluminescence from Er^{3+} ions in a-SiN alloys, *Phys. Rev. B* 59 (1999) 10091–10098, <https://doi.org/10.1103/>

- [6] C.T.M. Ribeiro, M. Siu Li, A.R. Zanatta, Spectroscopic study of Nd-doped amorphous SiN films, *J. Appl. Phys.* 96 (2004) 1068–1073, <https://doi.org/10.1063/1.1760843>.
- [7] Z. Yuan, D. Li, M. Wang, D. Gong, P. Cheng, P. Chen, D. Yang, Photoluminescence of Tb³⁺ -doped SiNx films with different Si concentrations, *Mater. Sci. Eng. B* 146 (2008) 126–130, <https://doi.org/10.1016/j.mseb.2007.07.023>.
- [8] Z. Yuan, D. Li, M. Wang, P. Chen, D. Gong, L. Wang, D. Yang, Photoluminescence of Tb³⁺ doped SiNx films grown by plasma-enhanced chemical vapor deposition, *J. Appl. Phys.* 100 (2006) 83106, <https://doi.org/10.1063/1.2358301>.
- [9] J.A. Guerra, L. Montañez, A. Winnacker, F. De Zela, R. Weingärtner, Thermal activation and temperature dependent PL and CL of Tb doped amorphous AlN and SiN thin films, *Phys. Status Solidi Curr. Top. Solid State Phys.* 12 (2015) 1183–1186, <https://doi.org/10.1002/pssc.201400226>.
- [10] M. Milosevic, S.L. Berets, A.Y. Fadeev, Single-reflection attenuated total reflection of organic monolayers on silicon, *Appl. Spectrosc.* 57 (2003) 724–727, <https://doi.org/10.1366/000370203322005454>.
- [11] J.M. Ramírez, J. Wojcik, Y. Berencén, P. Mascher, B. Garrido, On the photoluminescence of as-deposited Tb-doped silicon oxides and oxynitrides fabricated by ECR-PECVD, in: L. Vivien, S. Honkanen, L. Pavesi, S. Pelli, J.H. Shin (Eds.), *International Society for Optics and Photonics*, 2014, p. 913309, <https://doi.org/10.1117/12.2052571>.
- [12] G. Scardera, T. Puzzer, G. Conibeer, M.A. Green, Fourier transform infrared spectroscopy of annealed silicon-rich silicon nitride thin films, *J. Appl. Phys.* 104 (2008) 104310, <https://doi.org/10.1063/1.3021158>.
- [13] O. Debieu, R.P. Nalini, J. Cardin, X. Portier, J. Perrière, F. Gourbilleau, Structural and optical characterization of pure Si-rich nitride thin films, *Nanoscale Res. Lett.* 8 (2013) 31, <https://doi.org/10.1186/1556-276X-8-31>.
- [14] M. Lattemann, E. Nold, S. Ulrich, H. Leiste, H. Holleck, Investigation and characterisation of silicon nitride and silicon carbide thin films, *Surf. Coatings Technol.* 174–175 (2003) 365–369, [https://doi.org/10.1016/S0257-8972\(03\)00695-9](https://doi.org/10.1016/S0257-8972(03)00695-9).
- [15] F. Giorgis, F. Giuliani, C.F. Pirri, E. Tresso, C. Summonte, R. Rizzoli, R. Galloni, A. Desalvo, P. Rava, Optical, structural and electrical properties of device-quality hydrogenated amorphous silicon-nitrogen films deposited by plasma-enhanced chemical vapour deposition, *Philos. Mag. B* 77 (1998) 925–944, <https://doi.org/10.1080/13642819808206395>.
- [16] S. Zhou, W. Liu, C. Cai, H. Liu, Comparative investigation of infrared optical absorption properties of silicon oxide, oxynitride and nitride films, in: J. Chu, Z. Wang (Eds.), *International Society for Optics and Photonics*, 2010, p. 79950T, <https://doi.org/10.1117/12.888194>.
- [17] G. Zatyrb, A. Podhorodecki, J. Serafińczuk, M. Motyka, M. Banski, J. Misiewicz, N.V. Gaponenko, Optical properties of Tb and Eu doped cubic YAlO₃ phosphors synthesized by sol-gel method, *Opt. Mater. (Amst.)* 35 (2013) 2090–2094, <https://doi.org/10.1016/j.optmat.2013.05.026>.
- [18] A. Podhorodecki, G. Zatyrb, J. Misiewicz, J. Wojcik, P.R.J. Wilson, P. Mascher, Green light emission from terbium doped silicon rich silicon oxide films obtained by plasma enhanced chemical vapor deposition, *Nanotechnology* 23 (2012) 475707, <https://doi.org/10.1088/0957-4484/23/47/475707>.
- [19] J.M. Ramírez, J. Wojcik, Y. Berencén, A. Ruiz-Caridad, S. Estradé, F. Peiró, P. Mascher, B. Garrido, Amorphous sub-nanometre Tb-doped SiO_xN_y/SiO₂ superlattices for optoelectronics, *Nanotechnology* 26 (2015) 85203, <https://doi.org/10.1088/0957-4484/26/8/085203>.
- [20] Y.-T. An, C. Labbé, J. Cardin, M. Morales, F. Gourbilleau, Highly efficient infrared quantum cutting in Tb³⁺ - Yb³⁺ codoped silicon oxynitride for solar cell applications, *Adv. Opt. Mater.* 1 (2013) 855–862, <https://doi.org/10.1002/adom.201300186>.
- [21] J.A. Guerra, F. De Zela, K. Tucto, L. Montañez, J.A. Töfflinger, A. Winnacker, R. Weingärtner, Effect of thermal annealing treatments on the optical activation of Tb³⁺ -doped amorphous SiC:H thin films, *J. Phys. D: Appl. Phys.* 49 (2016) 375104, <https://doi.org/10.1088/0022-3727/49/37/375104>.
- [22] S.V. Deshpande, E. Gulari, S.W. Brown, S.C. Rand, Optical properties of silicon nitride films deposited by hot filament chemical vapor deposition, *J. Appl. Phys.* 77 (1995) 6534–6541, <https://doi.org/10.1063/1.359062>.
- [23] O. Blázquez, J. López-Vidrier, L. López-Conesa, M. Busquets-Masó, S. Estradé, F. Peiró, S. Hernández, B. Garrido, Structural and optical properties of Al-Tb/SiO₂ multilayers fabricated by electron beam evaporation, *J. Appl. Phys.* 120 (2016) 135302, <https://doi.org/10.1063/1.4964110>.
- [24] A. Sillen, Y. Engelborghs, The correct use of average fluorescence parameters, *Photochem. Photobiol.* 67 (1998) 475–486, <https://doi.org/10.1111/j.1751-1097.1998.tb09082.x>.
- [25] J.R. Lakowicz, *Principles of Fluorescence Spectroscopy*, Springer, 2006.
- [26] F. Benz, H.P. Strunk, J. Schaab, U. Künecke, P. Wellmann, Tuning the emission colour by manipulating terbium-terbium interactions: terbium doped aluminum nitride as an example system, *J. Appl. Phys.* 114 (2013) 073518, <https://doi.org/10.1063/1.4818815>.
- [27] A. Polman, D.C. Jacobson, D.J. Eaglesham, R.C. Kistler, J.M. Poate, Optical doping of waveguide materials by MeV Er implantation, *J. Appl. Phys.* 70 (1991) 3778–3784, <https://doi.org/10.1063/1.349234>.
- [28] J. Michel, J.L. Benton, R.F. Ferrante, D.C. Jacobson, D.J. Eaglesham, E.A. Fitzgerald, Y.-H. Xie, J.M. Poate, L.C. Kimerling, Impurity enhancement of the 1.54- μ m Er³⁺ luminescence in silicon, *J. Appl. Phys.* 70 (1991) 2672–2678, <https://doi.org/10.1063/1.349382>.
- [29] Y.S. Tang, K.C. Heasman, W.P. Gillin, B.J. Sealy, Characteristics of rare-earth element erbium implanted in silicon, *Appl. Phys. Lett.* 55 (1989) 432–433, <https://doi.org/10.1063/1.101888>.
- [30] A.J. Kenyon, C.E. Chryssou, C.W. Pitt, T. Shimizu-Iwayama, D.E. Hole, N. Sharma, C.J. Humphreys, Broad-band and flashlamp pumping of 1.53 μ m emission from erbium-doped silicon nanocrystals, *Mater. Sci. Eng. B* 81 (2001) 19–22, [https://doi.org/10.1016/S0921-5107\(00\)00677-2](https://doi.org/10.1016/S0921-5107(00)00677-2).
- [31] E. Steveler, H. Rinnert, M. Vergnat, Low-temperature photoluminescence properties of Nd-doped silicon oxide thin films containing silicon nanocrystals, *J. Lumin.* 183 (2017) 311–314, <https://doi.org/10.1016/j.jlumin.2016.11.048>.
- [32] A. Podhorodecki, G. Zatyrb, L.W. Golacki, J. Misiewicz, J. Wojcik, P. Mascher, On the origin of emission and thermal quenching of SRSO:Er³⁺ films grown by ECR-PECVD, *Nanoscale Res. Lett.* 8 (2013) 1–12, <https://doi.org/10.1186/1556-276X-8-98>.
- [33] L. Zhang, H. Jin, W. Yang, Z. Xie, H. Miao, L. An, Optical properties of single-crystalline α -Si₃N₄ nanobelts, *Appl. Phys. Lett.* 86 (2005) 061908, <https://doi.org/10.1063/1.1862753>.
- [34] C. Di Valentin, G. Palma, G. Pacchioni, Ab initio study of transition levels for intrinsic defects in silicon nitride, *J. Phys. Chem. C* 115 (2011) 561–569, <https://doi.org/10.1021/jp106756f>.
- [35] H. Aozasa, I. Fujiwara, Y. Kamigaki, Analysis of carrier traps in silicon nitride film with discharge current transient spectroscopy, photoluminescence, and electron spin resonance, *Jpn. J. Appl. Phys.* 46 (2007) 5762–5766, <https://doi.org/10.1143/JJAP.46.5762>.
- [36] P. Dorenbos, The 4f_n→4f_n – 15d transitions of the trivalent lanthanides in halogenides and chalcogenides, *J. Lumin.* 91 (2000) 91–106, [https://doi.org/10.1016/S0022-2313\(00\)00197-6](https://doi.org/10.1016/S0022-2313(00)00197-6).
- [37] Y.Q. Li, N. Hirotsaki, R.-J. Xie, T. Takeda, M. Mitomo, Photoluminescence properties of rare earth doped α -Si₃N₄, *J. Lumin.* 130 (2010) 1147–1153, <https://doi.org/10.1016/j.jlumin.2010.02.012>.
- [38] A. Podhorodecki, L.W. Golacki, G. Zatyrb, J. Misiewicz, J. Wang, W. Jadwisienczak, K. Fedus, J. Wojcik, P.R.J. Wilson, P. Mascher, Excitation mechanism and thermal emission quenching of Tb ions in silicon rich silicon oxide thin films grown by plasma-enhanced chemical vapour deposition—do we need silicon nanoclusters? *J. Appl. Phys.* 115 (2014) 143510, <https://doi.org/10.1063/1.4871015>.
- [39] G. Zatyrb, M.M. Klak, J. Wojcik, J. Misiewicz, P. Mascher, A. Podhorodecki, Effect of hydrogen passivation on the photoluminescence of Tb ions in silicon rich silicon oxide films, *J. Appl. Phys.* 118 (2015), <https://doi.org/10.1063/1.4939199>.
- [40] Z. Huang, Z. Wang, H. Yuan, J. Zhang, F. Chen, Q. Shen, L. Zhang, Synthesis and photoluminescence of doped Si₃N₄ nanowires with various valence electron configurations, *J. Mater. Sci.* 53 (2018) 13573–13583, <https://doi.org/10.1007/s10853-018-2330-4>.
- [41] A. Podhorodecki, P. Gluchowski, G. Zatyrb, M. Syperek, J. Misiewicz, W. Lojkowski, W. Strek, Influence of pressure-induced transition from nanocrystals to nanoceramic form on optical properties of Ce-doped Y₃Al₅O₁₂, *J. Am. Ceram. Soc.* 94 (2011) 2135–2140, <https://doi.org/10.1111/j.1551-2916.2010.04374.x>.